Analytical Biochemistry 446 (2014) 9–18

Contents lists available at ScienceDirect

Analytical Biochemistry

journal homepage: www.elsevier.com/locate/yabio

Fabrication of a highly sensitive disposable immunosensor based on indium tin oxide substrates for cancer biomarker detection

Mehmet Çetin Canbaz, Mustafa Kemal Sezgintürk *

Division of Biochemistry, Department of Chemistry, Faculty of Science, Namık Kemal University, Tekirdağ, Turkey

ARTICLE INFO

Article history:
Received 7 August 2013
Received in revised form 7 October 2013
Accepted 9 October 2013
Available online 17 October 2013

Keywords:
Cancer biomarkers
Biosensor
HER-3
ITO
Single frequency impedance

ABSTRACT

Anti-HER-3 antibody was used for the first time in a disposable immunosensor based on indium tin oxide (ITO) substrate for HER-3 quantification. Anti-HER-3 was immobilized onto ITO substrate by 3-aminopropyl)triethoxysilane (APTES) and glutaraldehyde. This highly sensitive immunosensor was capable of detecting concentrations of HER-3 down to the femtogram/ml level by investigating changes in the charge transfer resistance (R_{ct}) using electrochemical impedance spectroscopy (EIS). Construction of ITO layers was carefully investigated using a broad range of techniques such as voltammetry, EIS, atomic force microscopy (AFM), and scanning electron microscopy (SEM). Meanwhile, in an immunosensor system, the "single frequency impedance" technique was first used for characterization of interaction between HER-3 and anti-HER-3. Eventually, the proposed ITO-based immunosensor was applied to artificial serum samples spiked with HER-3.

HER-3 is a type of transmembrane growth factor receptor of the human epidermal growth factor receptor. It can activate intracellular signaling pathways in response to extracellular signals [1,2]. HER-3 itself is an incomplete receptor functionally, and consequently it is a dependent protein [3]. Many studies have reported that tumor progression and reduced survival of patients with breast [4], ovarian [5], and pancreatic [6] cancers, gastric carcinoma [7], malignant melanoma and metastases [8], and head and neck squamous cell carcinoma were considerably associated with overexpression of HER-3. Moreover, HER-3 overexpression is importantly correlated with poor prognosis [9] and worse metastasis-free survival [10] in colorectal carcinomas. For instance, it has been revealed that both HER-3 messenger RNA and protein were upregulated in human breast cancers, such that in human breast cancers HER-3 overexpression has been reported in the ratio of 50–70% [11,4,12]. In addition, it seems to be associated with metastasis and local recurrence [13,14].

In this study, because of the vital importance of HER-3, an immunosensor based on indium tin oxide (ITO)[1] substrate as a working electrode was developed. Because of its good electrical conductivity, ITO is one of the most widely used transparent conducting oxides. Transparent ITO thin films on flexible substrates such as polyethylene terephthalate (PET) have many applications. It has been reported that they can be used in plastic liquid crystal display devices, transparent electromagnetic shielding materials, flexible electro-optical devices, heat reacting mirrors, and the like [15]. Various ITO-based immobilization techniques have led to new applications in the construction of biosensors. For example, gold nanoparticles were self-assembled onto an ITO electrode to prepare a modified sandwich-type electrochemical immunoassay platform for determination of vascular endothelial growth factor [16]. In another study, ITO was covered by a poly(dopamine) layer for biomolecule immobilization [17]. However, for more reliable and stable biosensor systems based on ITO substrates, more developments are needed to create useful immobilization strategies.

Electrochemical impedance spectroscopy (EIS) has become an efficient method that is used for many chemical and physical processes. Hence, it is quite often applied in fabrication of immunosensors. In a typical EIS-based immunosensor, after any biorecognition event, charge transfer resistance (R_{ct}) usually increases, and this change in R_{ct} can be used for detection of any substances. However, in this study, a novel impedance method was applied to the immunosensor for the first time. "Single frequency impedance" was performed to reveal binding characteristics between HER-3 and anti-HER-3.

The focus of this study was on a simple immobilization procedure for anti-HER-3, development of a highly sensitive and disposable HER-3 biosensor, and its impedimetric characterization. The current study is the first to use anti-HER-3 as a bioreceptor in an immunosensor system for HER-3 analysis. We also identified

* Corresponding author. Fax: +90 282 250 99 25.
E-mail addresses: msezginturk@nku.edu.tr, msezginturk@hotmail.com (M.K. Sezgintürk).

[1] *Abbreviations used:* ITO, indium tin oxide; PET, polyethylene terephthalate; EIS, electrochemical impedance spectroscopy; SEM, scanning electron microscopy; BSA, bovine serum albumin; APTES, 3-aminopropyltriethoxysilane; CV, cyclic voltammetry; AFM, atomic force microscopy; SAM, self-assembled monolayer.

0003-2697/$ - see front matter © 2013 Elsevier Inc. All rights reserved.
http://dx.doi.org/10.1016/j.ab.2013.10.014

scanning electron microscopy (SEM) features of the surfaces of each layer based on a combination of EIS in the presence of $[Fe(CN)_6]^{3-/4-}$ as a redox couple. Certain working parameters such as anti-HER-3 concentration and anti-HER-3 binding period were optimized and characterized. Finally, the immunosensor was applied to artificial serum samples for the determination of HER-3.

Materials and methods

Reagents and material

All reagents were purchased from Sigma–Aldrich (St. Louis, MO, USA). ITO-coated substrates (ITO-coated PET film) were obtained from Sigma–Aldrich. The surface resistivity and transmittance were 60 ohm/square and 550 nm (>79%), respectively. HER-3 and anti-HER-3 were also purchased from Sigma–Aldrich. HER-3, anti-HER-3, and 0.1% bovine serum albumin (BSA) were prepared in a phosphate buffer (50 mM, pH 7.0). Solutions of HER-3, anti-HER-3 and 0.1% BSA were stored at 20 °C until use. Synthetic serum solution was prepared by using 4.5 mM KCl, 5 mM $CaCl_2$, 4.7 mM D(+)-glucose, 2.5 mM urea, 0.1% human serum albumin, and 145 mM NaCl. A redox probe solution was prepared in a phosphate buffer (50 mM, pH 7.0) that contained 0.1 M KCl, 5 mM $Fe(CN)_6^{4-}$, and 5 mM $Fe(CN)_6^{3-}$.

Apparatus

Electrochemical experiments were carried out by using a Gamry potentiostat/galvanostat (Reference 600, Gamry Instruments, Warminster, PA, USA) interfaced with a PC via an EChem Analyst containing physical electrochemistry, pulse voltammetry, and EIS software (Gamry Instruments). A sheet of ITO substrate (2×15 mm) was used as a working electrode, and a silver/silver chloride reference electrode and platinum wire counter electrode were obtained from BASi (West Lafayette, IN, USA).

Fabrication of ITO-based impedimetric immunosensors

The first step was cleaning of the ITO substrates. The ITO substrates were cleaned using the following procedure. After sonication in acetone, soap solution, and ultra-pure water for 10 min each, they were dried under a stream of argon. After that, the clean ITO substrates were immersed in ultra-pure water containing hydrogen peroxide (1:7, v/v) and ammonium hydroxide (1:7, v/v) for 1 h to form hydroxyl groups on the surface of the ITO substrates in a dark and cool atmosphere. Then, the substrates were washed with ultra-pure water and dried with argon gas gently. During the next step, the ITO surface was modified with 3-aminopropyltriethoxysilane (APTES) to introduce amino terminals for covalent attachment of anti-HER-3 antibody. For this purpose, the ITO substrate was dipped into the APTES solution (1%) overnight. For covalent interaction between anti-HER-3 and ITO modified with APTES, a crosslinking agent, glutaraldehyde (0.1%), was used next. Afterward, an ITO sheet modified with anti-HER-3 was immersed in ultra-pure water to remove physically adsorbed anti-HER-3 molecules. Finally, the ITO substrate was immersed in the solution of BSA (0.1%) to block active ends. The bare (cleaned) and modified ITO substrates were denoted as ITO, ITO/APTES, ITO/APTES/anti-HER-3, ITO/APTES/anti-HER-3/BSA, and ITO/APTES/anti-HER-3/BSA/HER-3.

Experimental measurements

Cyclic voltammetry (CV) was used to characterize the steps of electrode modification and immobilization. The applied potential was varied between −500 and 500 mV (step size: 20 mV; scan rate: 50 mV/s) in the presence of a 5-M $[Fe(CN)_6^{4-}]/[Fe(CN)_6^{3-}]$ (1:1) solution that served as a redox probe containing 0.1 M KCl. For electrochemical impedance studies, an alternating wave of 10-mV amplitude was applied to the electrode over the formal potential of the redox couple (0 V). The redox couple used for the impedance studies was the same as that used for CV. Impedance spectra were collected in the frequency range between 10,000 and 0.05 Hz.

SEM and AFM studies

Structural observations of a surface modified by immobilization and HER-3 binding were performed by a field emission scanning electron microscope (FEI-Quanta FEG 250 model at 10,000-fold magnification) at the Scientific and Technological Research Center of Namık Kemal University (NABİLTEM). An acceleration voltage of 5 kV was used to acquire SEM images.

Atomic force microscopy (AFM) studies were performed by using an AFM Plus model microscope (NanoMagnetics Instruments, Turkey). Measurements were carried out by using silicon cantilevers (PPPNCLR-50 [PointProbe Plus non-contact], Nanosensors, Switzerland). Topographic images were taken in tapping mode in air and collected at a scan rate of 20 nm/s with a scan size of 40×40 and 2×2 μm.

Results and discussion

Immobilization of anti-HER-3 onto ITO sheets

The first and perhaps most important step was cleaning of the ITO surface because the further modification of ITO would definitely not have been realized without this cleaning procedure. The cleaning step mentioned above removed organic contaminants from the ITO surface, and removing these contaminants also increased the conductivity. Nevertheless, it was possible to continue immobilization after the cleaning step. All of these steps were characterized by the help of EIS and CV. A well-defined characteristic voltammogram of the redox couple, $Fe(CN)_6^{3-/4-}$, was observed on the ITO modified with hydroxyl groups. Fig. 1A shows the cyclic voltammograms obtained for the immobilization steps of anti-HER-3.

As is shown in Fig. 1A, the characteristic cyclic voltammograms of the redox couple $Fe(CN)_6^{3-/4-}$, which exhibits a nearly reversible electrode reaction without any complications of proceeding or post-chemical reactions, were not observed for the unmodified ITO surface because of its high electrical resistivity. After cleaning of the surface by the procedure mentioned above, the peak currents of the redox probe did not change considerably. However, the formation of hydroxyl groups on the ITO surface resulted in an obvious increase in anodic and cathodic currents compared with the previous ITO surfaces. This effect was probably caused by increasing the electron transfer rate of the redox probe. The ITO surface modified with hydroxyl groups was then activated with APTES, leaving a primary amine group on the surface. Most likely, these amino ends electrostatically actuated the redox probe toward the working electrode, and consequently the peak currents increased considerably. After covalent attachment of anti-HER-3, both the cathodic and anodic peak currents were decreased dramatically due to the hindering effect of anti-HER-3 on the electron transfer rate. During this process, glutaraldehyde was subsequently used to react with the amine group, yielding an aldehyde that could form an imine linkage with the primary amine group on anti-HER-3. During the last step, the addition of BSA that blocked free active ends also caused a further decrease in peak

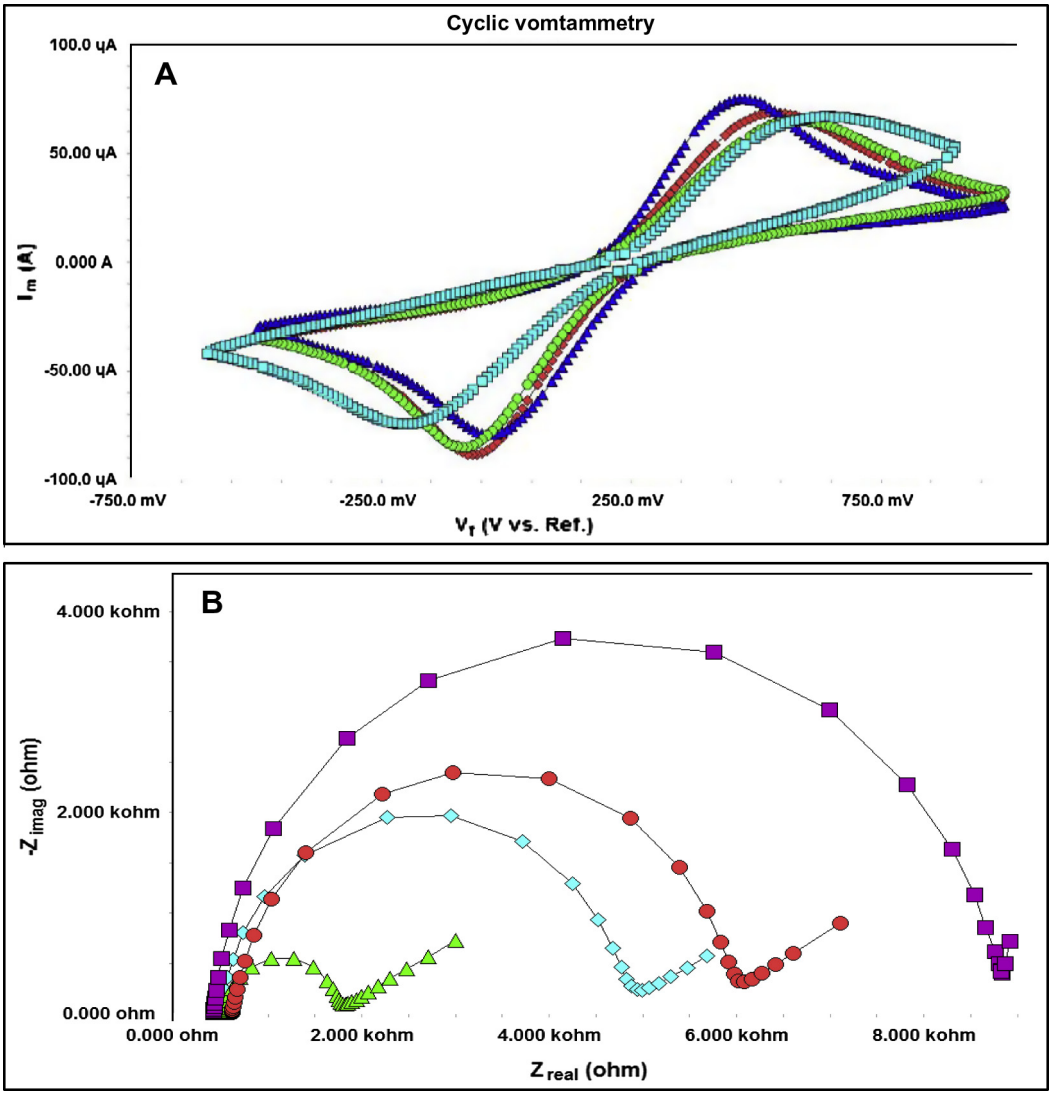

Fig.1. Electrochemical characterization of ITO-based immunosensor. (A) Cyclic voltammograms of anti-HER-3 immobilization by covalent attachment. (B) Electrochemical impedance spectra of HER-3 immobilization steps: ■, ITO/OH; ▲, ITO/APTES; ♦, ITO/APTES/anti-HER-3; ●, ITO/APTES/anti-HER-3/BSA.

currents due to its insulator protein structure. That is to say, modification of the ITO surface by an insulator protein made it more resistant to redox probe diffusion. After binding HER-3, a significant decrease was observed in anodic and cathodic peak currents. This again was caused by slowing of the electron transfer rate by HER-3 proteins.

Fig. 1B shows a typical Nyquist diagram of impedance spectra belonging to all fabrication steps in the frequency range from 0.05 to 10,000 Hz. The semicircular portion observed at high frequencies corresponds to the limited electron transfer process, whereas the linear part represents the limited diffusion process. EIS is one of the most important techniques for characterization of electrode surfaces and presents analytic solutions for many processes. Besides these, identification of membranes, biosensor characterization, and fabrication can also be effectively monitored by EIS. Conversely, enzyme–substrate interactions after antigen–antibody, receptor–ligand, or DNA–DNA interactions can be identified with the help of EIS. In Nyquist plots, the complex impedance is displayed as the sum of the real and imaginary components (Z_{real} and Z_{imag}, respectively), the semicircle diameter at higher frequencies corresponds to the electron transfer resistance (R_{et}), and the linear part at lower frequencies corresponds to the diffusion process (Warburg impedance). The diameter of the semicircle also exhibited the blocking behavior of the modified electrode after each modification step. The electrochemical impedance data were fitted with an equivalent circuit model by using commercial software called Gamry Echem Analyst, shown in Fig. 2.

This equivalent circuit model consisted of resistive and capacitive elements as well as a Warburg element. R_s was the resistance of the working solution, and the C_{dl} (constant phase element) was

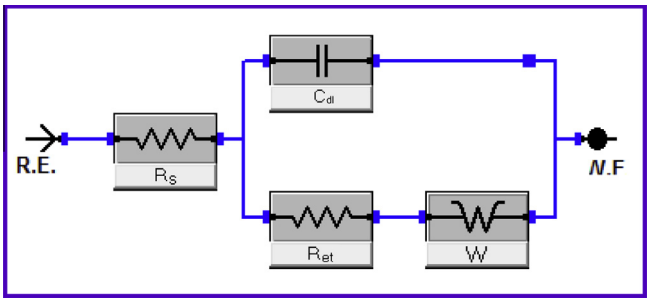

Fig.2. Equivalent circuit model applied to fit the impedance measurements. R_s, ohmic resistance of electrolyte solution; C_{dl}, associated with double layer capacitance; R_{et}, electron transfer resistance; W, Warburg impedance.

connected with the capacitance of the complex bioactive layer. R_{ct} was related to the electron transfer resistance through the electrode surface, and the Warburg impedance, Z_w, described the normal diffusion to the electrode surface through the complex layer. The experiments revealed that the results showed excellent agreement between CV and EIS studies. During the formation step of hydroxyl groups onto cleaned ITO sheets, the impedance spectra also showed that hydroxyl groups formed on the electrode surface did not considerably affect the electron transfer resistance of the surface. That is to say, in this case the hydroxyl groups did not cause a dramatic alteration in the diffusion of the redox probe to electrode surface. The charge transfer resistance (R_{ct}) values were decreased significantly in self-assembled monolayer (SAM) formation of APTES on the ITO substrate owing to formation of amino ends, which might help the redox probe to diffuse onto the electrode surface. Immobilization of anti-HER-3 onto the ITO electrode modified with APTES via glutaraldehyde gave rise to an increase in R_{ct} values. In this case, anti-HER-3 probably exhibited higher resistances against the diffusion of redox probe molecules. Similarly, blocking of active free aldehyde ends by BSA increased the electrical resistivity of the electrode surface. Consequently, the BSA layer acted as an effective diffusion barrier to the charge transfer reactions. It can be concluded that a good linear relationship between semicircle diameters and electrode layers indicates successful construction of the biosensor. A schematic representation of the immobilization steps is given in Scheme 1.

Optimization studies of HER-3 biosensor

To accurately conduct optimization studies requires assays that are extremely sensitive and highly discerning. Therefore, optimization of the immobilization steps was extremely important. For this purpose, the parameters such as concentration of anti-HER-3 used for immobilization, anti-HER-3 incubation period needed for optimal immobilization performance, and HER-3 incubation periods for detection were optimized. First, it was shown that impedimetric and voltammetric methods are powerful tools for studying the immobilization and measurement steps through the biosensor preparation and HER-3 analysis stages.

The APTES SAM has been widely used in many different applications. In this study, first the surface of ITO was cleaned and then –OH ends were introduced on ITO surface. After that, ITO/OH was modified with a SAM of APTES, which was bounded with anti-HER-3 with the help of a crosslinking agent, glutaraldehyde, by forming a strong amide linkage at both ends with free available amino groups of APTES and anti-HER-3. To obtain the optimal results during this process, the first parameter, the concentration of anti-HER-3, was investigated in detail. To determine the effect of anti-HER-3 concentrations on immobilization performance and biosensor response, different biosensor systems were constructed by using 5-, 20-, 40-, and 80-pg/μl anti-HER-3 portions. It can be seen from the results (Fig. 3) that both the peak currents and electron transfer resistance values were affected by the concentration of anti-HER-3.

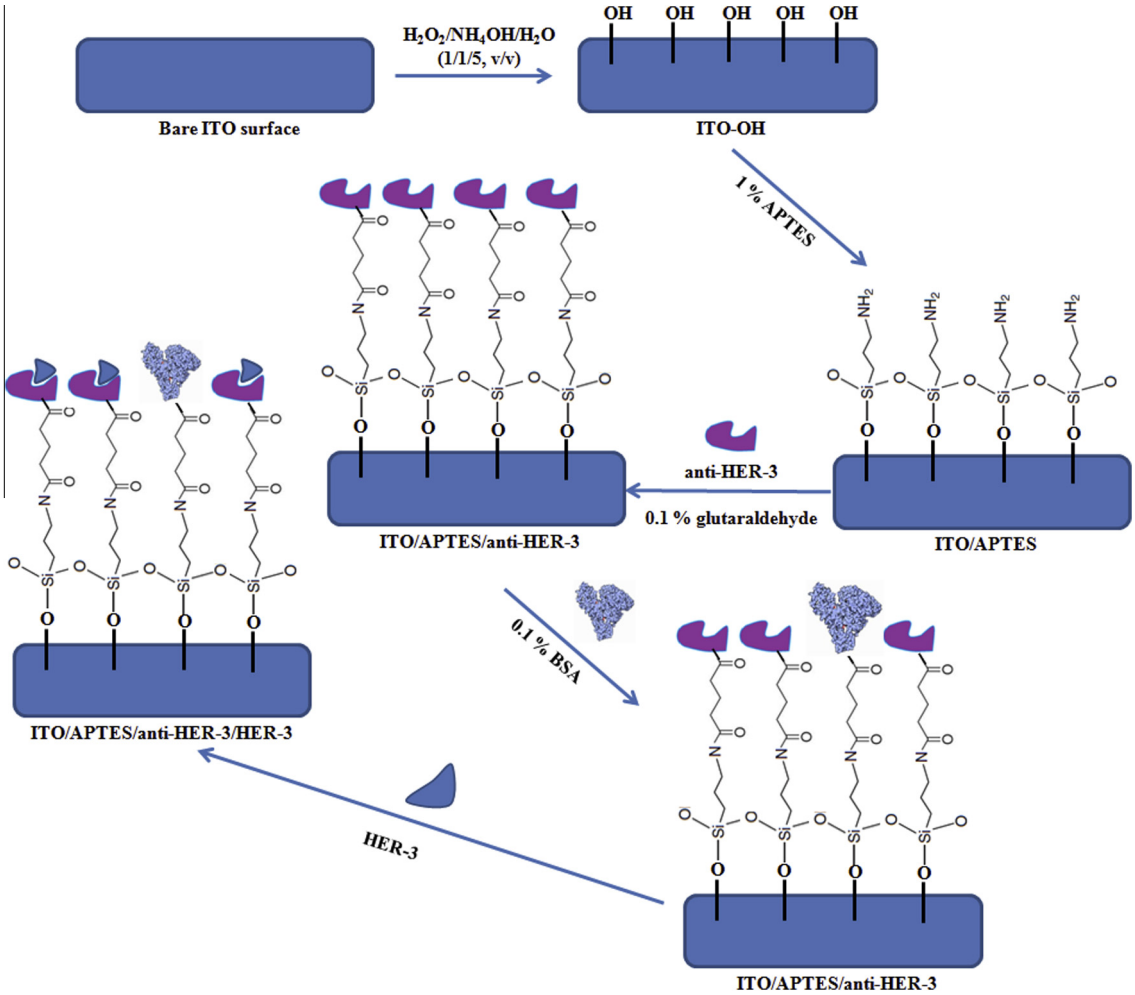

Scheme 1. Covalent immobilization steps of anti-HER-3 onto ITO substrates.

HER-3 calibration curves drawn by using different anti-HER-3 concentrations showed that levels of anti-HER-3 lower than 40 pg/μl were not sufficient to obtain good and valid results. Most likely, the reason was because, with low concentrations of anti-HER-3 on the surface, HER-3 did not bind sufficiently, which allowed the redox probe to diffuse easily through the electrode surface. By this process, the electron transfer resistance cannot reach the expected degree. However, the charge transfer resistance differences of the calibration curve belonging to the biosensor built up with 80 pg/μl anti-HER-3 were slightly higher than the biosensor built up with 40 pg/μl anti-HER-3. Hence, although the electron transfer resistances of 80 pg/μl anti-HER-3 were slightly higher than those of 40 pg/μl anti-HER-3, the optimal anti-HER-3 concentration was 40 pg/μl anti-HER-3. Using high concentrations of anti-HER-3 was unnecessary in terms of increasing biosensor signals.

The next important parameter was the incubation period for anti-HER-3 immobilization. Anti-HER-3 was crosslinked to amino ends of APTES SAM by glutaraldehyde (0.1%). The glutaraldehyde compound provides the most popular and versatile method for labeling or crosslinking to amino ends. For identifying the optimal crosslink ratio and immobilization performance of anti-HER-3, different incubation periods (30, 45, 60, and 90 min) were used to fabricate biosensors, thereby clarifying the influence of anti-HER-3 incubation durations on biosensor responses. The experiments showed that the response of the biosensor would be influenced by the period of anti-HER-3 incubation during immobilization. HER-3 calibration curves obtained by the impedance spectra related to these findings can be seen in Fig. 4A.

The experiments revealed that an increase in the period of incubation of anti-HER-3 gave rise to unfavorable results. The cyclic voltammograms and impedance spectra belonging to these experiments can also be seen in Fig. 4B and C. When anti-HER-3 was immobilized by using a period of 30 min, the resulting immunosensor provided insignificant signals that could not be evaluated. R_{ct} values (obtained for 80 fg/ml HER-3) for the incubation periods for 45, 60, and 90 min were 1629, 2873, and 1915 ohm, respectively. An increase in the incubation period of anti-HER-3 increased the charge transfer resistance to longer than 60 min. This result was expected because of the blocking behavior of the anti-HER-3 layer on the electrode surface for the redox probe $[Fe(CN)_6]^{3-/4-}$, which was reflected in the impedance spectroscopy as an increase in the diameter of the semicircle at high frequencies. However, the charge transfer resistances (R_{ct}) decreased considerably with an increase in incubation times of more than 60 min. At the end of the 90-min incubation period, anti-HER-3 solution on the electrode surface completely evaporated spontaneously, although the ITO-based electrode was incubated in a moisture medium. Most likely, the immobilization performance of anti-HER-3 was negatively affected due to the long period of incubation. Moreover, a long period of incubation with glutaraldehyde should have resulted in a denaturation of the three-dimensional structure of anti-HER-3 protein. Consequently, even if anti-HER-3 is immobilized on the ITO surface, it cannot bind its ligand, HER-3, because of this denaturation effect. It seemed that incubation periods shorter than 90 min caused the solution of anti-HER-3 to evaporate partially. However, incubation periods longer than 60 min led to a decrease in biosensor signals. In this condition, it is conceivable that the signals decreased because of insufficient crosslinking activity of glutaraldehyde. This was an expected result because a crosslinking process of short duration is not expected to be effective for crosslinking of anti-HER-3 to the electrode surface. Therefore, 60 min was chosen as the optimal incubation period for anti-HER-3 immobilization.

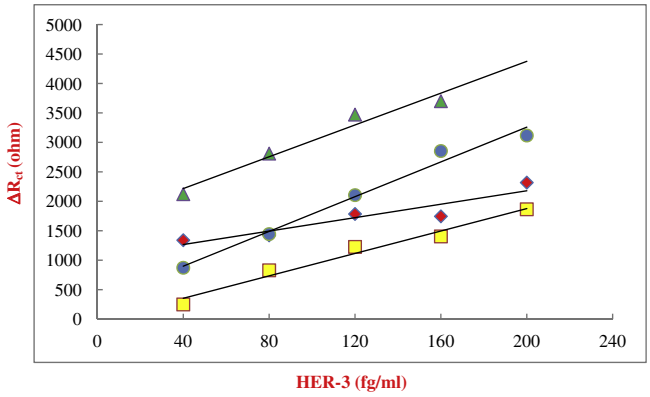

Fig.3. HER-3 calibration graphs for ITO-based immunosensors constructed by immobilization of different anti-HER-3 concentrations. Anti-HER-3 concentrations used in the construction of the biosensors were varied from 5 to 80 pg/μl. HER-3 calibration graphs obtained for these biosensors are shown by the following: ♦, 5 pg/μl; ■, 20 pg/μl; ●, 40 pg/μl; ▲, 80 pg/μl.

Eventually, the incubation period for binding between anti-HER-3 and HER-3 was optimized. For this purpose, anti-HER-3/HER-3 interaction was realized by using different incubation periods such as 30, 45, 60, and 90 min. The results obtained in the studies of optimization for HER-3 incubation periods were very similar to those of anti-HER-3. The binding ratio of HER-3 to anti-HER-3 decreased with an increase in incubation periods. This was probably caused by an effect similar to that in anti-HER-3 incubation. Because of that, the most effective period for HER-3 incubation was 60 min. Similarly, HER-3 incubation periods shorter than 60 min resulted in a decrease in charge transfer resistances. In this condition, the biosensor signals were probably decreased because there was insufficient interaction between HER-3 and anti-HER-3 immobilized on ITO substrates. Finally, if anti-HER-3 and HER-3 incubation periods are evaluated in terms of total measurement duration, short periods for both incubation processes should be favorable.

SEM and AFM characterization studies

SEM and AFM techniques were very useful tools to obtain information about the morphological characteristics of the resulting different surfaces of the biosensor during each step of the fabrication process. SEM was used to characterize the surface morphologies of the proposed biosensor layers (Fig. 5A). Bare ITO substrate showed a homogeneous surface (Fig. 5A1), whereas an anti-HER-3 modified surface had almost uniform granular morphology attributed to the dispersion of anti-HER-3 protein onto the ITO surface (Fig. 5A2). On application of BSA used for blocking active ends of surface, the granular morphology of anti-HER-3 changed into the more globular form (Fig. 5A3) due to the three-dimensional structure of BSA. Fig. 5A4 shows more aggregation than Fig. 5A3 because of the interaction between anti-HER-3 and HER-3.

In AFM imaging studies, using contact mode for proteins was ineffective because the protein structures were changed and damaged by the cantilever tip to which proteins attached during the imaging process, leading to unreliable and irreproducible images [18]. Fig. 5B shows AFM images taken during one of the immobilization steps. Bare ITO sheet had a homogeneous rough surface morphology (Fig. 5B1), and in further steps the immobilization of anti-HER-3 (Fig. 5B2) and the last HER-3 binding (Fig. 5B3) implied further alteration of surface morphologies. Eventually, the results obtained with SEM and AFM were in good agreement with those obtained from impedance characterization studies.

Analytical characteristics of ITO-based anti-HER-3 biosensor

In this study, EIS was used mainly to determine the variation of diffusion rate of a redox probe associated with changes in the

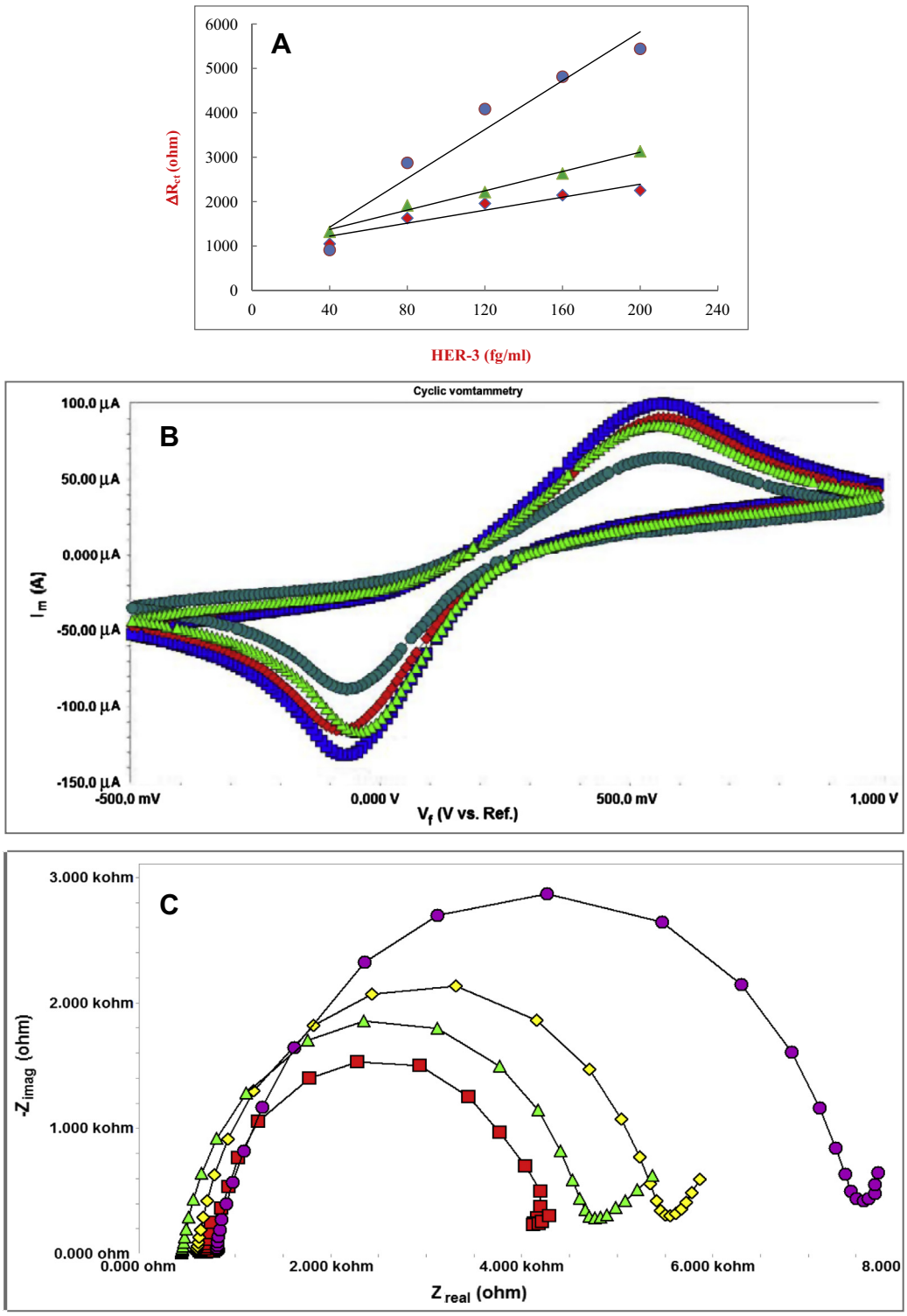

Fig.4. Effect of anti-HER-3 binding period on ITO-based immunosensor. (A) HER-3 calibration graphs obtained by using biosensors prepared with different anti-HER-3 binding periods: ■, 30 min; ♦, 45 min; ●, 60 min; ▲, 90 min. (B) Cyclic voltammograms obtained for biosensors constructed by different anti-HER-3 binding periods: ■, 30 min; ♦, 45 min; ●, 60 min; ▲, 90 min. (C) Impedance spectra obtained for biosensors constructed by different anti-HER-3 binding periods: ■, 30 min; ♦, 45 min; ●, 60 min; ▲, 90 min. In all CV and EIS studies, 80 fg/ml HER-3 was used.

electron transfer resistance related to HER-3 concentration. The charge transfer resistances related to the HER-3 concentrations were calculated with the help of the equivalent circuit model given in Fig. 2. To obtain a calibration curve of the biosensor, the variation of the absolute impedance calculated by the following equation was used:

$$\Delta R_{ct} = R_{ct(\text{anti-HER-3/HER-3})} - R_{ct(\text{anti-HER-3})}$$

where $R_{ct(\text{anti-HER-3/HER-3})}$ is the value of the charge transfer resistance after anti-HER-3 was coupled to HER-3 and $R_{ct(\text{anti-HER-3})}$ is the value of the charge transfer resistance when anti-HER-3 was immobilized on the electrode. As can be seen from Fig. 6A, peak

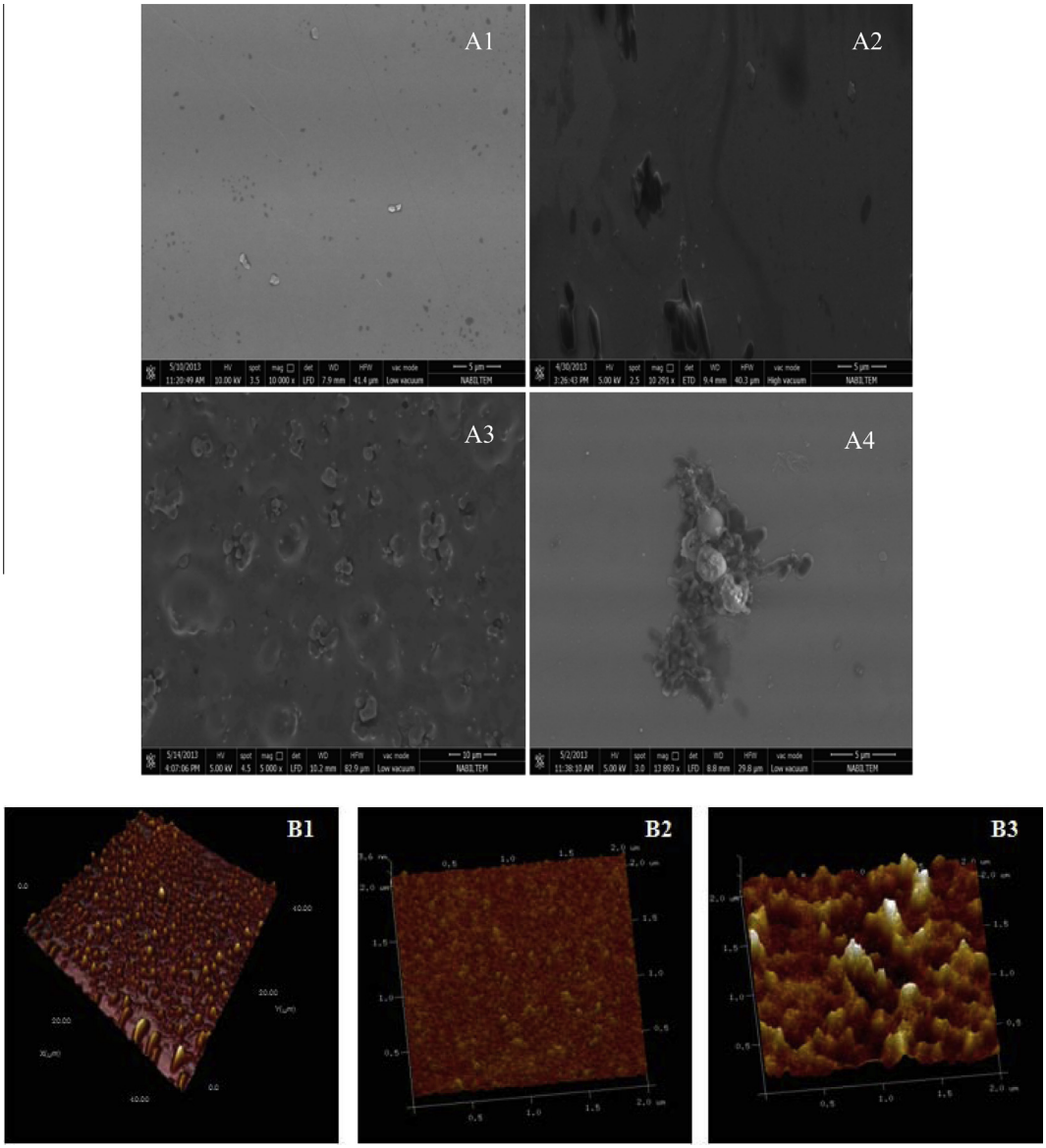

Fig.5. SEM and AFM characterization of the biosensor surfaces. SEM images: A1 (10,000 magnitude), bare ITO; A2 (20,291 magnitude), ITO/APTES/anti-HER-3; A3 (5000 magnitude), ITO/APTES/anti-HER-3/BSA; A4 (13,893 magnitude), ITO/APTES/anti-HER-3/BSA/HER-3. AFM images: B1 (scanning area 0–40 μm), bare ITO; B2 (scanning area 0–2 μm), ITO/APTES/anti-HER-3; B3 (scanning area 0–2 μm), ITO/APTES/anti-HER-3/BSA/HER-3.

currents decreased with the increase in the concentrations of HER-3 standard solutions.

Fig. 6B shows the Nyquist plot evaluation of the ITO-based immunosensor for different HER-3 concentrations. It was observed that the semicircle diameter in the Nyquist plots increased with increasing HER-3 concentrations. Moreover, the low frequencies could used for concentration-dependent measurements.

The increment of HER-3 concentration increased the charge transfer resistance (R_{ct}), achieving a linear range between 40 and 200 fg/ml. A calibration graph for HER-3 was prepared with the help of the differences in charge transfer resistances after HER-3 binding. The calibration curve is given in Fig. 7.

The reproducibility of the HER-3 immunosensor was identified by the help of eight biosensors fabricated using the same set of procedures. HER-3 calibration graphs were prepared and evaluated by using these biosensors. As indicated by the results obtained, the immunosensor reported here had good reproducible characteristics. As a result, the ITO-based immunosensor can be used for HER-3 detection and quantification. The linear detection ranges of eight biosensors for HER-3 were the same between 40 and 200 fg/ml. The results are summarized in Table 1.

Repeatability is another factor that must be determined, especially for an immunosensor. The repeatability of the presented ITO-based immunosensor should be defined as the degree of single biosensor that could be used continually for a series of measurements with the same concentration of HER-3. The charge transfer resistances of the biosensor were investigated when it was consecutively exposed to a 40-fg/ml HER-3 standard solution 10 times. The repeatability of the measurements was very good considering that the correlation coefficient of the measurements was 5.9%, and the average value and standard deviation were calculated as 40.6 and 2.4 fg/ml, respectively.

Moreover, in this study, a new impedimetric technique was also applied to the biosensor for the first time. In the literature, EIS is used for the immobilization and characterization of a biosensor. It is also used to analyze the charge transfer resistances of a modified surface. To characterize the binding of HER-3 to anti-HER-3 that was immobilized on the ITO surface, the single frequency

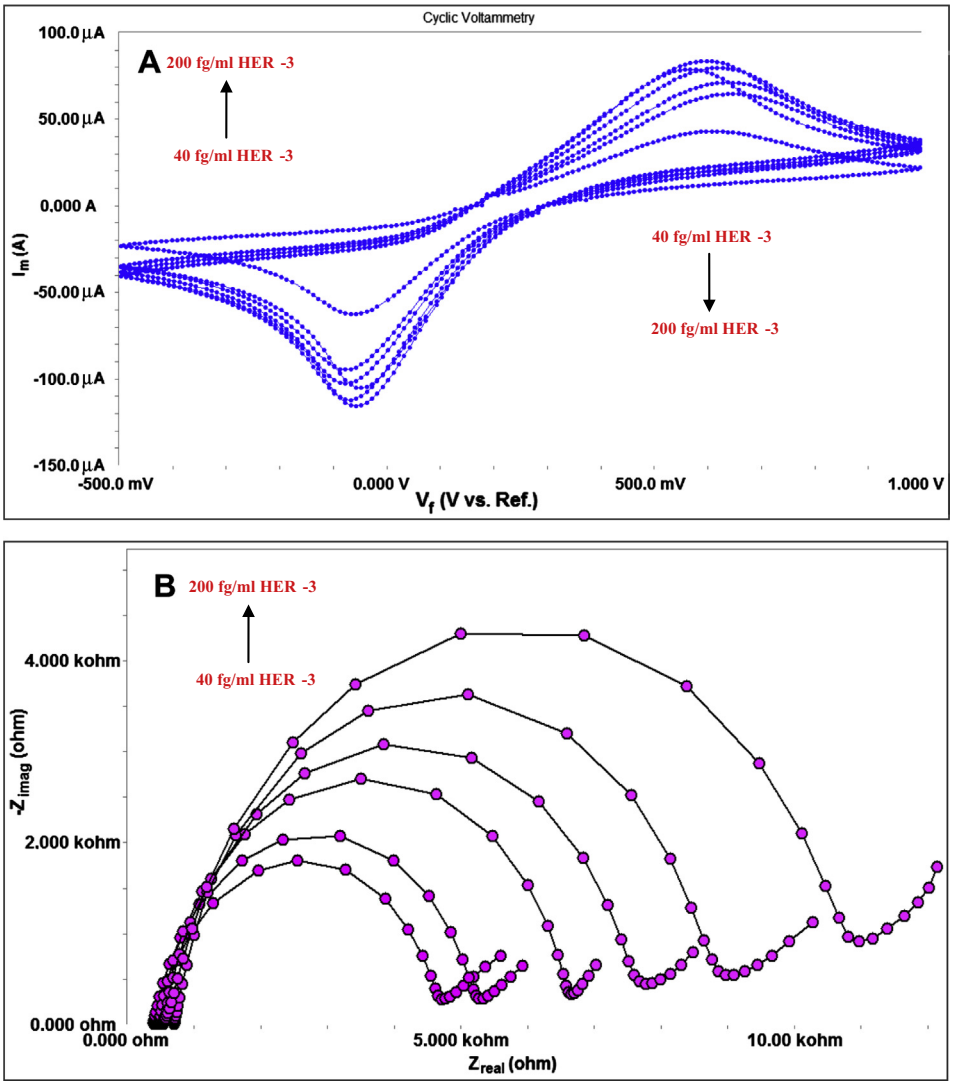

Fig.6. Cyclic voltammograms (A) and impedance spectra (B) obtained for different concentrations of HER-3 by ITO-based anti-HER-3 immunosensor.

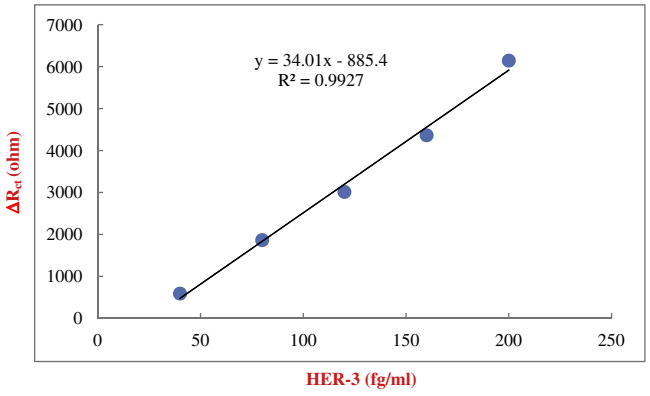

Fig.7. HER-3 calibration curve obtained by ITO-based immunosensor.

impedance technique was first performed successfully. As is known in electrochemistry, to discover surfaces of working electrodes, several methods such as SEM, scanning tunneling microscopy, and scanning reference electrodes should be operated. However, using these methods to potential is commonly time-consuming and requires expensive equipment. Moreover, SEM and AFM should also be used for surface characterization of the biosensors. As is well known, both of these instruments are extremely expensive, and in any laboratory SEM/AFM should not be provided. Consequently, as a valuable alternate method, measurements can be performed across the electrode at a single frequency to create an image of the electrode or, alternatively, can be performed at a

Table 1
Results for reproducibility and sample analysis.

(A) Reproducibility of the biosensor

Biosensor number	R^2	y	Linear range (fg/ml)
1	0.9845	$15.185x + 4$	40–200
2	0.9854	$16.785x + 872$	40–200
3	0.9808	$23.609x + 274.9$	40–200
4	0.9934	$13.048x + 954.9$	40–200
5	0.9893	$10.24x + 2042.6$	40–200
6	0.9911	$25.115x + 155.8$	40–200
7	0.9882	$31.868x - 54.952$	40–200
8	0.9904	$32.863x - 790.7$	40–200

(B) HER-3 detection in artificial serum samples

Added	Found by biosensor	% Recovery	% Relative difference
40	40.8	102.0	2.0
80	81.3	101.6	1.6

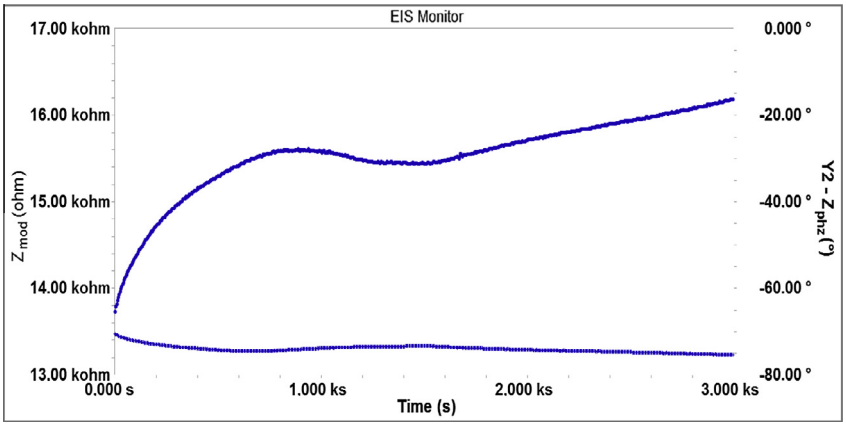

Fig.8. Single frequency impedance measurement.

given location to create a complete spectrum. In other words, single frequency impedance measurements can be performed to monitor the changes in the surfaces of the biosensors.

Single frequency impedance measures the impedance at a fixed frequency against time. Consequently, it should be possible to control the experiment with a repeat time and a total time. For this purpose, the potentiostat was set up at a fixed frequency of 5 Hz. The impedance was measured at this fixed frequency as a function of time and phase angle for 60 min. The result is shown in Fig. 8.

Single frequency impedance measurements were very informative about the binding of HER-3 to anti-HER-3. The significant change in the phase angle was due to interaction between HER-3 and anti-HER-3. In this experiment, the most important requirement was to give more attention to preventing environmental interference effects such as a possible electromagnetic wave, an inductive effect from the surrounding area, and magnetic stirring of the reaction cell that could cause an unstable electrode surface. Eventually, from the results, it should be concluded that single frequency impedance can be used for biosensor evaluation, process monitoring, or evaluating slow, time-dependent changes in a biosensor surface.

To investigate the storage stability of the ITO-based immunosensor, the immunosensors were stored at 4 °C for various periods such as 1, 2, 3, and 4 weeks. The biosensor response was constant for the first 3 weeks. However, the immunosensor stored for 4 weeks did not work at the end of the storage period, probably because of damage to the surface of the electrode. Despite this, it could be concluded that the storage stability studies of the immunosensor clarified that the long-term stability of the biosensor was reasonably good.

Finally, the artificial serum samples spiked with HER-3 were analyzed using the presented ITO-based immunosensor for the quantification of HER-3. Results from three different measurements were averaged (Table 1). The results presented here show that HER-3 levels of the artificial serum samples analyzed by the ITO-based immunosensor agreed with those of the spiked amount of HER-3 to the artificial serum samples.

Conclusions

In this study, a simple immobilization process was performed to prepare an impedimetric and disposable immunosensor for HER-3 quantification based on ITO substrates. Anti-HER-3 antibody was first used in this study for fabrication of an immunosensor integrated with ITO substrates. It was shown that SEM, AFM, and EIS investigations on different layers of the immunosensor were in good agreement with each other by the successful immobilization of anti-HER-3 and analysis of HER-3. Another goal of this study was to perform single frequency impedance experiments. Important data on the interaction between HER-3 and anti-HER-3 was obtained by the single frequency impedance studies. From this, it is highly recommended that single frequency impedance be performed for different biosensor applications such as evaluation and to clarify slow, time-dependent changes in a biosensor surface. Calibration studies were performed, and it was found that the disposable immunosensor gave a linear response to HER-3 over the range from 40 to 200 fg/ml. Finally, this biosensor was successfully applied to HER-3 analysis in artificial serum samples.

Acknowledgments

This work was financially supported by TÜBİTAK (Scientific and Technological Research Council of Turkey, project 109 T 172). In addition, we thank the Namık Kemal University Scientific Research Projects Fund (project NKUBAP.00.10.YL.13.03) and the Namık Kemal University Scientific and Technological Research Center.

References

[1] M.A. Lemmon, J. Schlessinger, Cell signaling by receptor tyrosine kinases, Cell 141 (2010) 1117–1134.
[2] N.E. Hynes, H.A. Lane, ERBB receptors and cancer: the complexity of targeted inhibitors, Nat. Rev. Cancer 5 (2005) 341–354.
[3] E. Tzahar, H. Waterman, X. Chen, G. Levkowitz, D. Karunagaran, S. Lavi, B.J. Ratzkin, Y. Yarden, A hierarchical network of interreceptor interactions determines signal transduction by Neu differentiation factor/neuregulin and epidermal growth factor, Mol. Cell Biol. 16 (1996) 5276–5287.
[4] R. Naidu, M. Yadav, S. Nair, M.K. Kutty, Expression of c-erbB3 protein in primary breast carcinomas, Br. J. Cancer 78 (1998) 1385–1390.
[5] B. Tanner, D. Hasenclever, K. Stern, W. Schormann, M. Bezler, M. Hermes, M. Brulport, A. Bauer, I.B. Schiffer, S. Gebhard, et al., ErbB-3 predicts survival in ovarian cancer, J. Clin. Oncol. 24 (2006) 4317–4323.
[6] H. Friess, Y. Yamanaka, M.S. Kobrin, D.A. Do, M.W. Büchler, M. Korc, Enhanced erbB-3 expression in human pancreatic cancer correlates with tumor progression, Clin. Cancer Res. 1 (1995) 1413–1420.
[7] M. Hayashi, M. Inokuchi, Y. Takagi, H. Yamada, K. Kojima, J. Kumagai, T. Kawano, K. Sugihara, High expression of HER3 is associated with a decreased survival in gastric cancer, Clin. Cancer Res. 14 (2008) 7843–7849.
[8] M. Reschke, D. Mihic-Probst, E.H. van der Horst, P. Knyazev, P.J. Wild, M. Hutterer, S. Meyer, R. Dummer, H. Moch, A. Ullrich, HER3 is a determinant for poor prognosis in melanoma, Clin. Cancer Res. 14 (2008) 5188–5197.
[9] A. Beji, D. Horst, J. Engel, T. Kirchner, A. Ullrich, Toward the prognostic significance and therapeutic potential of HER3 receptor tyrosine kinase in human colon cancer, Clin. Cancer Res. 18 (2012) 956–968.
[10] A. Ho-Pun-Cheung, E. Assenat, C. Bascoul-Mollevi, F. Bibeau, F. Boissière-Michot, D. Cellier, D. Azria, P. Rouanet, P. Senesse, M. Ychou, et al., EGFR and HER3 mRNA expression levels predict distant metastases in locally advanced rectal cancer, Int. J. Cancer 128 (2011) 2938–2946.
[11] C.M. Quinn, J.L. Ostrowski, S.A. Lane, D.P. Loney, J. Teasdale, E.A. Benson, C-erbB-3 protein expression in human breast cancer: Comparison with other tumour variables and survival, Histopathology 25 (1994) 247–252.

[12] N.L.P. Barnes, S. Khavari, G.P. Boland, A. Cramer, W.F. Knox, N.J. Bundred, Absence of HER4 expression predicts recurrence of ductal carcinoma in situ of the breast, Clin. Cancer Res. 11 (2005) 2163–2168.
[13] N.R. Lemoine, D.M. Barnes, D.P. Hollywood, C.M. Hughes, P. Smith, E. Dublin, S.A. Prigent, W.J. Gullick, H.C. Hurst, Expression of the ERBB3 gene product in breast cancer, Br. J. Cancer 66 (1992) 1116–1121.
[14] A. Travis, S.E. Pinder, J.F.R. Robertson, J.A. Bell, P. Wencyk, W.J. Gullick, R.I. Nicholson, D.N. Poller, R.W. Blamey, C.W. Elston, I.O. Ellis, C-erbB-3 in human breast carcinoma: expression and relation to prognosis and established prognostic indicators, Br. J. Cancer 74 (1996) 229–233.
[15] H. Kim, C.M. Gilmore, Electrical, optical, and structural properties of indium tin oxide thin films for organic light-emitting devices, J. Appl. Phys. 86 (1999) 6451–6461.
[16] K. Gang-Il, K. Kyung-Woo, O. Min-Kyu, S. Yun-Mo, Electrochemical detection of vascular endothelial growth factors (VEGFs) using VEGF antibody fragments modified AuNPs/ITO electrode, Biosens. Bioelectron. 25 (2010) 1717–1722.
[17] L.I.U. Hong-Ying, Z.H.U. Jun-Jie, Preparation of electrochemical immunosensor using gold nanoclusters as signal amplification labels, Chin. J. Anal. Chem. 41 (2013) 657–663.
[18] M. Barbadillo, E. Casero, M.D. Petit-Domínguez, L. Vázquez, F. Pariente, E. Lorenzo, Gold nanoparticles-induced enhancement of the analytical response of an electrochemical biosensor based on an organic–inorganic hybrid composite material, Talanta 80 (2009) 797–802.